Biomaterials 35 (2014) 6015–6025

Contents lists available at ScienceDirect

Biomaterials

journal homepage: www.elsevier.com/locate/biomaterials

The epigenetic promotion of osteogenic differentiation of human adipose-derived stem cells by the genetic and chemical blockade of histone demethylase LSD1

Wenshu Ge [a,b,1], Yunsong Liu [b,1], Tong Chen [b], Xiao Zhang [b], Longwei Lv [b], Chanyuan Jin [b], Yong Jiang [a], Lei Shi [c,**], Yongsheng Zhou [b,d,*]

[a] Department of General Dentistry II, Peking University School and Hospital of Stomatology, Beijing 100081, China
[b] Department of Prosthodontics, Peking University School and Hospital of Stomatology, Beijing 100081, China
[c] Tianjin Key Laboratory of Medical Epigenetics, Department of Biochemistry and Molecular Biology, Tianjin Medical University, Tianjin 300070, China
[d] National Engineering Laboratory for Digital and Material Technology of Stomatology, Peking University School and Hospital of Stomatology, Beijing 100081, China

ARTICLE INFO

Article history:
Received 3 February 2014
Accepted 12 April 2014
Available online 1 May 2014

Keywords:
Epigenetic drug
Human adipose-derived stem cells
Histone methylation
Osteogenic differentiation
Lysine-specific demethylase 1

ABSTRACT

Human adipose-derived stem cells (hASCs) are a highly attractive source in bone tissue engineering. It has become increasingly clear that chromatin regulators play an important role in cell fate determination. However, how osteogenic differentiation of hASCs is controlled by epigenetic mechanisms is not fully understood. Here we use genetic tools and chemical inhibitors to modify the epigenetic program of hASCs and identify lysine-specific demethylase 1 (LSD1), a histone demethylase that specifically catalyzes demethylation of di- and mono- methyl histone H3 lysine 4 (H3K4me2/1), as a key regulator in osteogenic differentiation of hASCs. Specifically, we demonstrated that genetic depletion of LSD1 with lentiviral strategy for gene knockdown promoted osteogenic differentiation of hASCs by cell studies and xenograft assays. At the molecular level, we found that LSD1 regulates osteogenesis-associated genes expression through its histone demethylase activity. Significantly, we demonstrated LSD1 demethylase inhibitors could efficiently block its catalytic activity and epigenetically boost osteogenic differentiation of hASCs. Altogether, our study defined the functional and biological roles of LSD1 and extensively explored the effects of its enzymatic activity in osteogenic differentiation of hASCs. A better understanding of how LSD1 influences on osteogenesis associated epigenetic events will provide new insights into the modulation of hASCs based cell therapy and improve the development of bone tissue engineering with epigenetic intervention.

1. Introduction

Human adipose-derived stem cells (hASCs), one type of mesenchymal stem cells, possess a high plasticity to differentiate into multiple lineages including cartilage, bone, muscle and adipose in the presence of appropriate signaling factors and culture conditions [1–5]. Currently, hASCs have become a highly attractive source in tissue engineering and cell-based therapy of damaged bone defects, spinal fusion and skeletal reconstruction bone [2,6,7]. The main reason lies in the fact that hASCs can be obtained easily from adipose tissues carrying a more abundant and accessible pool of mesenchymal stem cells with a less invasive and less expensive procedures [8–10].

The critical issue for application of stem cells in tissue engineering is the initiation and control of cellular differentiation in a precise and appropriate manner. Recent evidence suggests that epigenetic regulation including DNA methylation and histone modification plays a key role in fate maintenance and lineage commitment of embryonic stem cells as well as mesenchymal stromal/stem cells [11–16]. Slight variations of these epigenetic

* Corresponding author. Department of Prosthodontics, Peking University School and Hospital of Stomatology, 22 Zhongguancun South Avenue, Haidian District, Beijing 100081, China. Tel.: +86 10 82195370 (office); fax: +86 10 62173402.
** Corresponding author. Department of Biochemistry and Molecular Biology, Tianjin Medical University, 22 Qixiangtai Road, Tianjin 300070, China. Tel./fax: +86 22 83336997.
E-mail addresses: shilei@tmu.edu.cn (L. Shi), kqzhouysh@hsc.pku.edu.cn, kqzhouysh@gmail.com (Y. Zhou).
[1] These authors contributed equally to this work.

http://dx.doi.org/10.1016/j.biomaterials.2014.04.055
0142-9612/

components might result in the changes of local chromatin configuration or nuclear architecture, impose flexible but precise control over the expression of the important regulatory genes, and eventually influence on cell fate determination without changes of the DNA sequences. Unlike genetic alterations, epigenetic changes are reversible and accessible to be regulated, and as such, drugs that target critical epigenetic regulators in cell commitment or differentiation are being overwhelmingly investigated [17,18].

Lysine-specific demethylase 1 (LSD1/KDM1A) is a flavin adenine dinucleotide (FAD)-dependent amine oxidase that catalyzes mono- and di-methyl moieties removal from histone H3 lysine 4 (H3K4) [19–21]. Despite progress in understanding the dynamic histone methylation regulation and in revealing the diverse molecular interactions for LSD1, the biological function of LSD1 is just beginning to be uncovered. Recent studies have linked LSD1 to certain high-risk tumors [22–30]. Moreover, LSD1 has been identified as one of the chromatin regulators implicated in the control of early embryogenesis [15,31–33]. In addition, it was reported that LSD1 represses hematopoietic stem and progenitor cell signatures during blood cell maturation [34]. Indeed, within the framework of the so-called epigenetic therapies, there is a growing interest in LSD1 as a potential drug target [26,35–38]. However, whether histone methylation associated epigenetic events impacted by LSD1 and currently developed LSD1 inhibitors can contribute to mesenchymal stem cells differentiation as well as bone tissue engineering are largely unknown.

Here, our study focused on investigating the functional role and the molecular mechanism of histone H3K4 demethylase LSD1, especially its catalytic activity in osteogenic differentiation of hASCs.

2. Materials and methods

2.1. Cell culture, osteogenic induction and LSD1 inhibitors

Human adipose-derived stem cells (hASCs) were purchased from ScienCell Research Laboratories (San Diego, CA). Stem cells from 3 donors with different lot numbers of the third passage were used for the *in vitro* and *in vivo* experiments. All cell-based *in vitro* experiments were repeated in triplicate. Osteogenic differentiation was induced with Dulbecco's modified Eagle medium (DMEM) containing 10% fetal bovine serum, 100 IU/ml penicillin/streptomycin, 100 nM dexamethasone, 0.2 mM ascorbic acid and 10 mM β-glycerophosphate. Pargyline (Sigma, St. Louis, MO) at the concentration of 3 mM, and CBB1007 (Millipore, Billerica, MA) at the concentration of 10 μM, 20 μM and 50 μM were used to induce osteogenic differentiation of hASCs. The hASCs with vehicle or LSD1 inhibitor treatment were cultured for 14 days before collection.

2.2. Plasmid constructions

Wild-type human LSD1 (LSD1-wt) was amplified from pcDNA3-LSD1, a gift from Dr. Yan Wang (Tianjin Medical University). The amplicons were then digested using NotI and BsrgI endonuclease (Fermentas, Hanover, MD) and incorporated into the PITA lentiviral vector. The LSD1-mt (K661A) was created following standard point mutation procedures with PITA-LSD1-wt as template using the following primers (F: GATTTGGCAACCTTAACGCGGTGGTGTTGTGTTTTG; R: CAAAACACAACACCACCGCGTTAAGGTTGCCAAATC). LSD1 siRNA Sequence (GAGACAGACAAATACTTG) was designed by White Head Institute Online Server and the DNA oligoes (F: TGAGACAGACAAATACTTGATTCAAGAGATCAAGTATTTGTCTGTCTCTTTTTTC; R: TCGAGAAAAAA-GAGACAGACAAATACTTGATCTCTTGAATCAAGTATTTGTCTGTCTCA) were cloned into the pLL3.7 shuttle vector with an independent cassette encoding enhanced green fluorescent protein (EGFP). The control siRNA sequence is GATATGGGCTGAATACAA and the corresponding DNA oligoes sequences are F: TGATATGGGCTGAATACAAATTCAAGAGATTTGTATTCAGCCCATATCTTTTTTC; R: TCGAGAAAAAAGATATGGGCTGAATACAAATCTCTTGAATTTGTATTCAGCCCATATCA.

2.3. Lentiviral production and infection

The recombinant overexpression construct or shRNA construct, as well as three helper vectors (pMDLg/pRRE, pRSV-REV and pVSVG) were transiently transfected into HEK293T cells using Lipofectamine 2000 (Invitrogen, Carlsbad, CA) according to the manufacturer's instructions. The viral supernatants were collected 48 h later, clarified by filtration and concentrated by ultracentrifugation. The concentrated viruses were then used to infect hASCs of passage 3 at a multiplicity of infection (MOI) of 100 in the presence of 8 μg/ml polybrene (Sigma). Twenty four hours later, the lentiviral containing medium were removed and replaced with fresh growth medium. The proliferation medium was replaced with differentiation medium when cells grew up to 80%–90% of confluence and the differences of osteogenic differentiation ability between the experimental group and control group were examined.

2.4. Alkaline phosphatase (ALP) activity of hASCs

The hASCs were seeded in 6-well plates, and ALP activity was determined by staining with nitro blue tetrazolium (NBT) and 5-bromo-4-chroro-3-indolyl phosphate (BCIP). For quantification of ALP activity, cells seeded in 6-well plates were rinsed two times with phosphate-buffered saline (PBS), followed by trypsinization and then scraping in distilled water. This was followed by three cycles of freezing and thawing. ALP activity was determined at 405 nm using p-nitrophenyl phosphate (pNPP) as the substrate. Total protein contents were determined with the BCA method using the Pierce (Thermo Fisher Scientific, Rockford, IL, www.piercenet.com) protein assay kit in aliquots of the same samples, which were read at 562 nm and calculated against a series of bovine albumin (BSA) standards. Relative ALP activity to the control treatment was calculated after normalization to the total protein content.

2.5. Mineralization assays for hASCs

The hASCs were seeded in 6-well plates, and mineralization was determined by staining with Alizarin red S. To quantify matrix mineralization, Alizarin red S-stained cultures were incubated in 100 mM cetylpyridinium chloride for 1 h to solubilize and release calcium-bound Alizarin red S into the solution. The absorbance of the released Alizarin red S was measured at 562 nm. Relative Alizarin red S intensity to the control treatment was calculated after normalization to the total protein content.

2.6. In vivo implantation of hASCs and Bio-Oss collagen scaffold hybrids

The hASCs (1×10^6) infected with lentivirus carrying control siRNA or LSD1 siRNA, were trypsinized and re-suspended directly into DMEM. The cells were then incubated with 7 mm × 4 mm × 2 mm Bio-Oss Collagen® (Geistlich, GEWO GmbH, Baden–Baden, Germany) scaffolds for 1 h at 37 °C with gently shaking followed by centrifugation at 150 g for 5 min. The collected hASCs-seeded scaffolds were implanted into the dorsal subcutaneous space of the 4–6-weeks old, BALB/c homozygous nude (nu/nu) mice (Peking University Experimental Animal Center) that had been randomly divided into two groups ($n = 5$ per group). One transplantation site was prepared in each mouse and transplanted with either scaffolds carrying control hASCs or LSD1 knockdown hASCs. This study was approved by the Ethics Committee of the Peking University Health Science Center, Beijing, China (PKUSSIRB-2013023) and all animal experiments were performed in accordance with the institutional animal guidelines.

2.7. Analyses of bone formation in vivo

Specimens were harvested at eight weeks after implantation, and animals were sacrificed by CO_2 asphyxiation. The specimens taken as a whole were radiographed with digital radiographic apparatus (GE Senograph 2000D, USA). Gray scales of five specimens in each group were then analyzed with medical image analyzing software (Image J, NIH). The mean density of hASCs-scaffold complex was presented as mean ± S.D. The bone constructs were fixed in 4% paraformaldehyde and then decalcified for 10 days in 10% EDTA (pH 7.4). After decalcification, the specimens were dehydrated and subsequently embedded in paraffin. Sections (5 mm thickness) were stained with hematoxylin and eosin (H&E) and Masson's trichrome. Meanwhile, osteogenesis was evaluated with immunohistochemical analysis for osteopontin (OPN), osteocalcin (OC) and GFP (sp kit, Vector, Burlingame, CA, primary antibodies were purchased from Santa Cruz Biotechnology, CA). Specimens were processed using identical protocols. For quantification of bone-like tissue, 3 images of each sample (15 images for each group) were taken randomly by microscope (Olympus, Tokyo, Japan) and Image-Pro Plus software (Media Cybernetics, Rockville, MD) was used to measure the area of new bone formation (osteoid or organized extracellular matrix) versus total area or mean density (total density of positive staining/cell containing tissue area) of immunohistochemical staining. Box-plot was used to exhibit the semi-quantitative results.

2.8. RNA extraction, reverse transcription, and quantitative real-time PCR

Total cellular RNAs from hASCs cultured in proliferation or differentiation medium for 14 days were isolated with Trizol reagent (Invitrogen, Carlsbad, CA) and used for first strand cDNA synthesis with the Reverse Transcription System (Promega, Madison, WI). Quantifications of all gene transcripts were performed by real-time RT-PCR using a Power SYBR Green PCR Master Mix and an ABI PRISM 7300 sequence detection system (Applied Biosystems, Foster City, CA) with the expression of *GAPDH* detected as the internal control. The primers used were: *ALP*, (forward) 5′-ATGGGATGGGTGTCTCCACA-3′ and (reverse) 5′-CCACGAAGGGGAACTTGTC-3′; *OC*, (forward) 5′-CACTCCTCGCCCTATTGGC-3′ and (reverse) 5′-CCCTCCTGCTTGGACACAAAG-3′; *OSX*, (forward) 5′-CCTCTGCGGGACTCAACAAC-3′ and (reverse) 5′-TAAAGGGGGCTGGATAAGCAT-3′; RUNX2, (forward) 5′-CCGCCTCAGTGATTTAGGGC-

3′ and (reverse) 5′- GGGTCTGTAATCTGACTCTGTCC-3′; LSD1, (forward) 5′-TGACCGGATGACTTCTCAAGA-3′ and (reverse) 5′-GTTGGAGAGTAGCCTCAAATGTC-3′; GAPDH, (forward) 5′-GAAGGTGAAGGTCGGAGTC-3′ and (reverse) 5′-GAAGATGGTGATGGGATTTC-3′. The cycle threshold values (*Ct* values) were used to calculate the fold differences by the ΔΔ*Ct* method.

2.9. Chromatin immunoprecipitation (ChIP) assay

The ChIP assay was performed as previously described [39–41]. Briefly, the hASCs (1×10^6) infected with lentivirus carrying control siRNA or LSD1 siRNA were cultured in differentiation medium for 0, 7 or 14 days. Then cells were cross-linked in 1% formaldehyde at 37 °C for 10 min and re-suspended in 200 μl lysis buffer [1% sodium dodecyl sulfate (SDS), 10 mM EDTA, and 50 mM Tris–HCl (pH 8.1)], and the nuclear lysates were sonicated and diluted 10-fold with immunoprecipitation buffer (16.7 mM Tris–HCl, pH 8.1; 167 mM NaCl; 1.2 mM EDTA; 0.01% SDS; and 1.1% Triton X-100). The lysates were then immunoprecipitated with non-specific rabbit IgG, H3K4me2, H3K4me1, LSD1 or H3 antibodies (Abcam, Cambridge, MA) for 12 h at 4 °C. Immune complexes were incubated with Protein G-Sepharose CL-4B (GE Healthcare, Piscataway, NJ) for 2 h at 4 °C. After successive washings, immune complexes containing DNA were purified and eluted, and the precipitated DNA was amplified by PCR. Primer pairs used in this study were as follows: *OC* promoter, (forward) 5′-AAATAGCCCTGGCAGATTCC-3′ and (reverse) 5′-CAGCCTCCAGCACTGTTTAT-3′; *OSX* promoter, (forward) 5′-CCGCTGGGAAAGCTGTAAT-3′ and (reverse) 5′-GAATGGGAGAATGGGAGAGAAG-3′. *GAPDH* promoter, (*forward*) 5′-TCTGCTCTGGGTGGTCATTGTGAA-3′ and (reverse) 5′-TGCTAAGTTTAGCCTGCCTGGTGA-3′ was used as a negative control.

2.10. Quantitative ChIP assays

The hASCs (1×10^6) infected with lentivirus carrying vector encoding control or LSD1 vector were cultured in proliferation or differentiation medium for 14 days. The collected ChIPed DNA from these cells or the cells treated with LSD1 inhibitor for 10 days under different culture conditions was Quantified by an ABI PRISM 7300 sequence detection system (Applied Biosystems, Foster City, CA) using a Power SYBR Green PCR Master Mix (Roche, Basel, Switzerland). Primer pairs used in this study were as follows: *OC* promoter, (forward) 5′-AAATAGCCCTGGCAGATTCC-3′ and (reverse) 5′-CAGCCTCCAGCACTGTTTAT-3′; *OSX* promoter, (forward) 5′-CCGCTGGGAAAGCTGTAAT-3′ and (reverse) 5′-GAATGGGAGAATGGGAGAGAAG-3′. Relative enrichment of LSD1 was normalized to the IgG of the control treatment after calculating the percentage of ChIPed DNA to the corresponding input, while the relative level of H3K4me2 or H3 was normalized to control treatment after calculating the percentage of ChIPed DNA to the corresponding input. The FLAG antibody used to immunoprecipitate FLAG-LSD1 in qChIP assays was got from Sigma (St. Louis, MO).

2.11. Statistical analysis

Data from triplicate *in vitro* experiments are presented as mean ± S.D. The Student's *t*-test was used for comparing two groups of data at $p < 0.05$ or $p < 0.01$ level of significance. Two-way analysis of variance (ANOVA) in conjugation with Tukey's test was used to compare multiple groups of data at $p < 0.05$ level of significance. All of the statistical testing results were determined by SPSS 20.0 (IBM, Armonk, NY) software.

3. Results

3.1. The effect of LSD1 depletion on osteogenic differentiation of hASCs in vitro

Previously, we showed that histone demethylase RBP2 (also known as KDM5A or JARID1A) suppresses the osteogenic potential of hASCs by modulating H3K4me3 status of key osteogenic genes [12]. To further explore the biological function of histone demethylase and to investigate the importance of the regulation of histone H3K4 methylation in bone tissue engineering field, the effect of histone demethylase LSD1 depletion on osteogenic differentiation of hASCs was first examined. The siRNA sequence against LSD1 was designed, and the corresponding DNA was constructed into the pLentilox lentivirus vector followed by lentiviral packaging. Subsequently, lentiviruses carrying control siRNA or LSD1 siRNA were infected into hASCs followed by culturing in proliferation medium (PM) or osteogenic differentiation medium (DM). To this end, alkaline phosphatase (ALP) staining and quantitative analyses were employed to test whether LSD1 plays a role in osteogenic differentiation of hASCs. The results in Fig. 1A demonstrated that the ALP activity of LSD1 deficient hASCs was significantly increased comparing with control siRNA treated cells when cultured in DM for the indicated periods. Furthermore, the extracellular matrix mineralization, as shown by Alizarin red S (ARS) staining and quantification was also markedly intensified in hASCs of LSD1 depletion compared with control cells when cultured in DM (Fig. 1B). The knockdown effect of LSD1 was examined by Western blotting (Fig. 1C). Taken together, these results indicated that LSD1 loss of function could promote osteogenic differentiation of hASCs *in vitro*.

3.2. The effect of LSD1 depletion on osteogenic differentiation of hASCs in vivo

To further investigate the role of LSD1 in osteogenic differentiation of hASCs, two types of hASCs that had either unchanged expression of LSD1 or specific knockdown of LSD1 expression (infected with lentivirus carrying control siRNA or LSD1 siRNA) were seeded in Bio-Oss Collagen scaffolds, and the hASCs-scaffold hybrids were implanted into the subcutaneous tissue of nude mice. Eight weeks after implantation, the hASCs-scaffold hybrids were harvested. Mineralization effect was then monitored by X-ray radiography *in vitro* and the gray scales of the specimens were further quantified. The results indicated that mean density of hASCs-scaffold with LSD1 knockdown was relatively higher comparing to control hybrids (Fig. 2A). Furthermore, histological examination corroborated the findings from X-ray radiography (Fig. 2B and C). The spotty area of osteoid marked with the structure of osteocyte lacunae or organized extracellular matrix with collagen fiber accumulation was examined by Hematoxylin and eosin (H&E) or Masson's trichrome staining, respectively (Fig. 2B and C). The positive osteoid structure indicated by black hollow arrows in HE staining (Fig. 2B) and collagen organization with green color (in the web version) in Masson's trichrome staining (Fig. 2C) were further quantified by histomorphometry analysis and the results indicated that the osteogenic differentiation potential of hASCs with LSD1 depletion was markedly increased, which is consistent with the observation from X-ray radiography. Meanwhile, immunohistochemistry staining and histomorphometry analysis showed that the LSD1 knockdown resulted in highly induced expression of osteogenic markers Osteocalcin (OC) and Osteopontin (OPN) (Fig. 2D). The dark brown granules (in the web version) marked by black hollow arrows indicated positive staining (Fig. 2D). To figure out whether the newly-formed bone was from the actual cells implanted or not, we checked the GFP protein expression (co-expressed with shRNA in the same pLentilox vector) by immunohistochemistry. We found that the bone-forming cells in the hybrids were positively stained, but not the adjacent fibrosis tissue (Fig. 2E). Taken together, these results from *in vivo* experiments further supported the notion that LSD1 functions to suppress osteogenic differentiation of hASCs.

3.3. Osteogenic genes expression upon LSD1 knockdown

The observation that LSD1 affects hASCs osteogenic differentiation triggers us to further test whether loss of function of LSD1 has an impact on osteogenic genes expression. To test this hypothesis, we compared the expression of osteogenic genes between the LSD1 knockdown group and control group in response to osteogenic stimulation. Total RNAs were extracted from lentivirus-infected hASCs cultured for 14 days in control or osteogenic condition and quantitative reverse transcription PCR (qRT-PCR) analyses were performed to measure the expression levels of osteogenic markers or/and key regulators *Alkaline phosphatase* (*ALP*), *Osteocalcin* (*OC*), *Osterix* (*OSX*) and *Runt-related transcription factor 2* (RU*NX2*). As

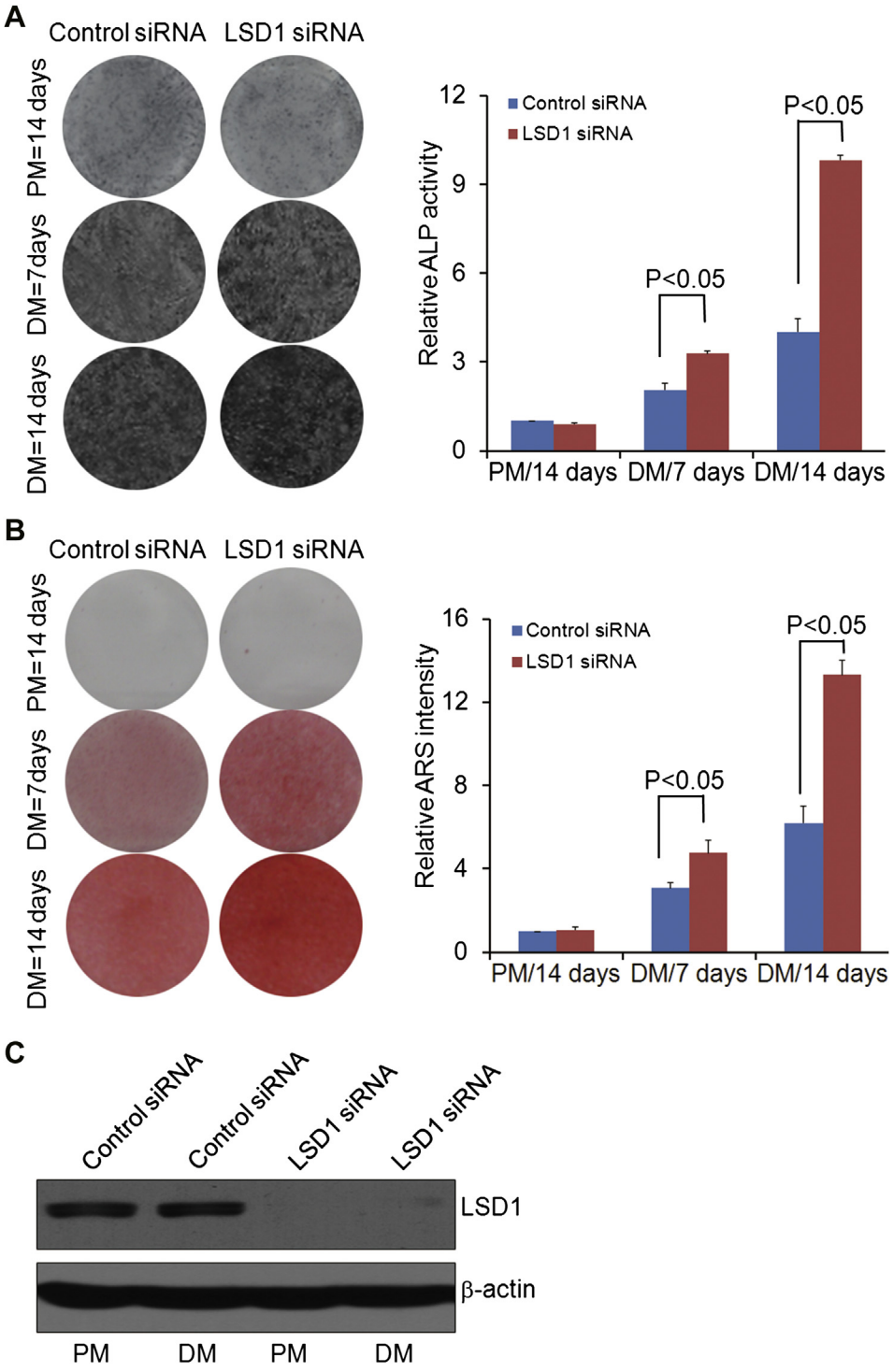

Fig. 1. LSD1 loss of function promotes osteogenic differentiation of hASCs *in vitro*. (A) ALP staining (left panel) and quantification (right panel) of hASCs infected with control or LSD1 knockdown viruses. (B) Alizarin red S (ARS) staining (left panel) and quantification (right panel) of hASCs infected with control or LSD1 knockdown viruses. (C) Validation of LSD1 knockdown effect by Western blotting with the indicated antibodies.

shown in Fig. 3A, comparing with the control siRNA treatment group, knockdown of LSD1 resulted in a marked increase of the mRNA expression levels of *ALP*, *OC*, *OSX* and *RUNX2*, although to variable extension. This observation indicated that promotion of osteogenic differentiation in LSD1 depletion cells was associated with increased expression of these osteogenic genes. The knockdown effect of LSD1 was examined by qRT-PCR as shown in Fig. 3B.

3.4. The H3K4me2/1 levels on promoters of osteogenic genes regulated by LSD1

To gain further insight into the physiological role of LSD1 during osteogenic differentiation of hASCs, we next examined whether LSD1 was directly involved in the regulation of osteogenesis associated genes. The recruitment of LSD1 on *OSX* and *OC*

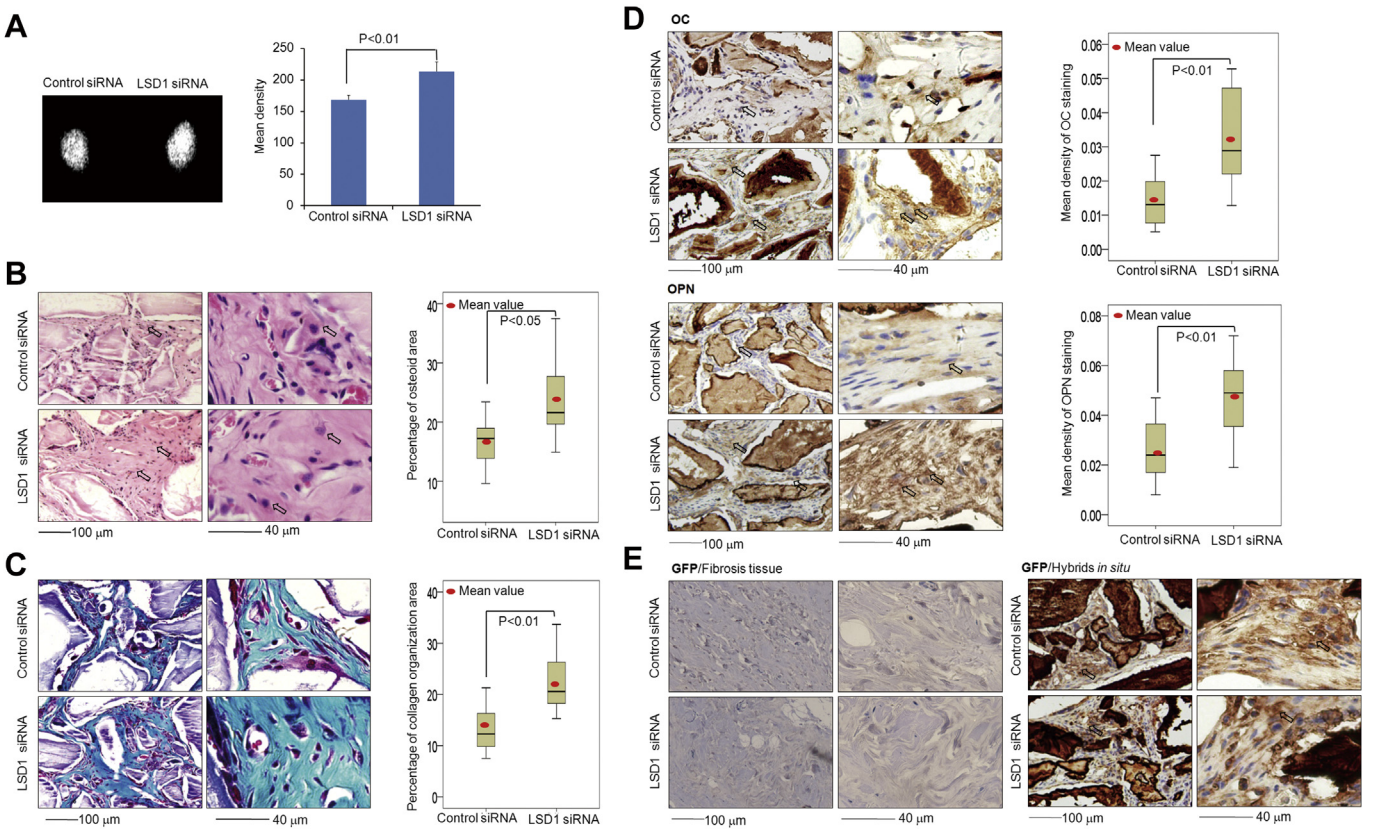

Fig. 2. LSD1 loss of function promotes osteogenic differentiation of hASCs *in vivo*. (A) X-ray radiography and quantification of implanted hASCs-scaffold complex. (B–D) H&E staining (B), Masson's trichrome staining (C) and immunohistochemistry (D) conjugated with histomorphometry analysis of histologic sections from implanted hASCs-scaffold hybrids. (E) Immunohistochemistry of GFP in histologic sections from implanted hASCs-scaffold hybrids and the adjacent fibrosis tissue. Low magnification images are provided in the left panel, while higher magnification images are in the right panels (B–E) of the stainings.

promoters was determined by Chromatin Immunoprecipitation (ChIP) assays in native (uninduced) or osteogenically-induced hASCs. These experiments revealed that LSD1 was highly enriched on the promoters of *OSX* and *OC*, but not that of *GAPDH* in native hASCs (Fig. 3C). Surprisingly, we found LSD1 enrichment decreased dramatically upon osteogenic induction (Fig. 3D). In addition, this diminishment of LSD1 occupancy was specifically and negatively correlated with increased levels of di- and mono-methylation of Histone H3 lysine 4 (H3K4me2/1), which are linked with transcriptionally active chromatin, whereas there were no changes in the levels of histone H3 incorporation (Fig. 3D). As stated before, LSD1 has been demonstrated to demethylate H3K4me2/1 in mammalian cells. In light of our observation that LSD1 influenced the expression of osteogenesis associated genes and its binding negatively correlated with H3K4me2/1 levels, it is logical to postulate that LSD1 may function to erase the H3K4me2/1 mark in the regulatory region of osteogenesis associated genes. In order to test this hypothesis, the levels of H3K4me2/1 at the promoters of osteogenesis associated genes were examined in hASCs with LSD1 knockdown upon osteogenic induction. Notably, compared with control lentivirus-infected cells, cells with loss-of-function of LSD1 displayed increased amounts of H3K4me2/1 on the *OSX* and *OC* promoters upon osteogenic induction, while the total histone H3 levels were not affected (Fig. 3D). However, in proliferation medium, the H3K4me2/1 mark remained at constantly low levels regardless of whether LSD1 was knocked down or not (Fig. 3D). Collectively, these data suggested that LSD1 occupy *OSX* and *OC* promoters to maintain the levels of H3K4me2/1.

3.5. LSD1 demethylase activity in hASCs osteogenic differentiation

To further address the functional significance of the enzymatic activity of LSD1, we next examined the effect of its catalytic mutant (K661A) on osteogenic differentiation of hASCs. Lentiviruses expressing empty control (vector), wild type LSD1 (LSD1-wt) and catalytic defective mutant LSD1 (LSD1-mt, K661A) were infected into hASCs, respectively, followed by culturing in proliferation or differentiation medium for 14 days. The stable cells were then collected and subjected to Alizarin red S staining and quantification. The results in Fig. 4A showed that LSD1-wt significantly reduced the ability of extracellular matrix mineralization of hASCs upon osteogenic induction, while LSD1-mt failed to do so. Meanwhile, overexpression of LSD1-wt resulted in a marked decrease of the mRNA expression levels of *ALP*, *OC*, *OSX* and *RUNX2*, but not that of LSD1-mt (Fig. 4B), indicating that the catalytic activity of LSD1 plays an essential role in regulating expression of these osteogenesis-related genes. Next, the overexpression effects and the correspondingly enzymatic activities of the LSD1-wt and LSD1-mt in stable hASCs were determined by Western blotting with indicated antibodies (Fig. 4C). The results indicated that LSD1-wt and LSD1-mt were equally expressed in hASCs, and K661A mutation (LSD1-mt) completely abrogated the histone demethylation activity of H3K4me2, a major substrate of LSD1 (Fig. 4C). To further test whether the catalytic activity of LSD1 contributes directly to the regulation of osteogenesis associated genes, we examined the recruitment of LSD1-wt and LSD1-mt on *OSX* and *OC* promoters *in vivo* with quantitative ChIP (qChIP) assays in hASCs of stably expressing FLAG tagged LSD1. We demonstrated that LSD1-wt and

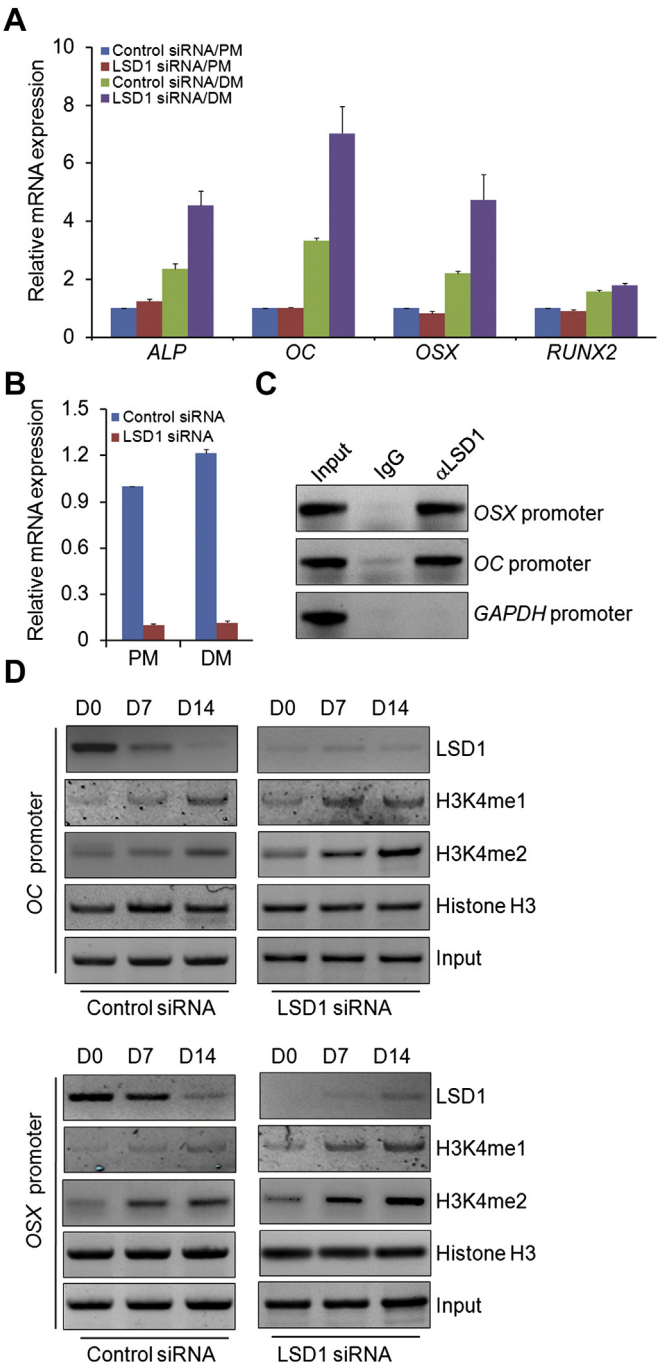

Fig. 3. LSD1 epigenetically governs osteogenesis associated genes expression. (A) qRT-PCR analysis of osteogenic genes expression in control and LSD1 depletion hASCs. (B) LSD1 knockdown effect was examined by qRT-PCR. (C) ChIP analysis of LSD1 recruitment to osteogenic genes *OSX* and *OC* promoters in hASCs cultured in proliferation medium. (D) ChIP analysis of H3K4me2 and H3K4me1 on *OSX* and *OC* gene promoters in hASCs cultured in different conditions with the indicated antibodies.

LSD1-mt could be equally recruited to and disassociated from *OC* and *OSX* promoters in a similar kinetics upon culture condition changing (Fig. 4D, left panel). Notably, compared with control lentivirus-infected cells, cells with gain-of-function of LSD1-wt displayed decreased amounts of H3K4me2 on the *OSX* and *OC* promoters upon osteogenic induction, while the total histone H3 levels were not affected (Fig. 4D, right panel). However, in cells with gain-of-function of LSD1-mt, the H3K4me2 mark remained at constantly high levels upon osteogenic induction (Fig. 4D, right panel). Collectively, these data indicated that the catalytic activity of LSD1 is essential to suppress osteogenic differentiation of hASCs.

3.6. The effect of LSD1 inhibitors on osteogenic differentiation of hASCs

Currently, the strategies of using small molecules to pharmaceutically inhibit the activity of LSD1 and epigenetically modulate gene expression are being under extensively investigated [37,42]. Therefore, we asked whether these inhibitors could be employed to target LSD1 and interfere with the osteogenic process in hASCs. First, hASCs were treated with pargyline hydrochloride, a monoamine oxidase (MAO) inhibitor [43]. The activity of ALP, as shown by ALP staining and quantification was augmented in hASCs treated with pargyline (Fig. 5A). The same is true when the extracellular matrix mineralization effect was determined by Alizarin red S staining and quantification (Fig. 5B). In addition, we showed that pargyline treatment resulted in a marked increase of *ALP* and *OSX* expression (Fig. 5C). Western blotting analysis demonstrated the level of H3K4me2 was significantly increased in the presence of pargyline in hASCs (Fig. 5D), indicating that the pargyline effect on hASCs was associated with impairment of LSD1enzymatic activity.

The fact that pargyline is a nonselective amine oxidase inhibitor and would result in potentially off-target effects [44,45], prompted us to further test the influence of another LSD1 bioactive chemical compound, CBB1007, that specifically inhibits demethylase activity of LSD1 on hASCs osteogenic differentiation. The ALP activity (Fig. 6A) and extracellular matrix mineralization effect (Fig. 6B) were both increased in CBB1007 treated hASCs in a dose dependent manner upon osteogenic differentiation without obviously cellular toxicity. Meanwhile, we demonstrated CBB1007 treatment resulted in a marked increase in the mRNA expression levels of *ALP*, *OC*, *OSX* and *RUNX2* in a dose dependent manner when compared with cells cultured in vehicle containing medium (Fig. 6C). Moreover, we demonstrated that the level of H3K4me2 was gradually increased and positively correlated with the concentration of CBB1007 in hASCs, although the level of histone H3 and the expression of LSD1 itself remained constantly unaffected (Fig. 6D). Interestingly, qChIP analysis demonstrated that CBB1007 treatment had no effect on LSD1 recruitment to *OC* and *OSX* promoters (Fig. 6E, left panel). However, hASCs exposed to CBB1007 treatment displayed increased amounts of H3K4me2 on the *OSX* and *OC* promoters upon osteogenic induction, while the total histone H3 levels were not affected (Fig. 6E, right panel). These observations indicated CBB1007 functions effectively to inhibit the catalytic activity of LSD1 both on genomic scale (examined by Western blotting) and gene specific promoters (examined by qChIP). Collectively, these data suggested that enzymatic inhibitors of LSD1 phenocopied the effects of LSD1 knockdown, confirming the specificity of this small molecule and further substantiating the notion that LSD1 suppresses osteogenic differentiation of hASCs through its catalytic activity.

4. Discussion

Here, we provide a strategy with genetic as well as epigenetic intervention to regulate osteogenic differentiation of hASCs. To characterize the function of histone demethylase LSD1 in osteogenic differentiation of hASCs, a combination of *in vitro* experiments were carried out. By quantifying ALP activity, matrix mineralization capacity and osteogenic gene expression profiles, which are common methods used in osteogenic differentiation studies, we found that LSD1 depletion could promote osteogenic

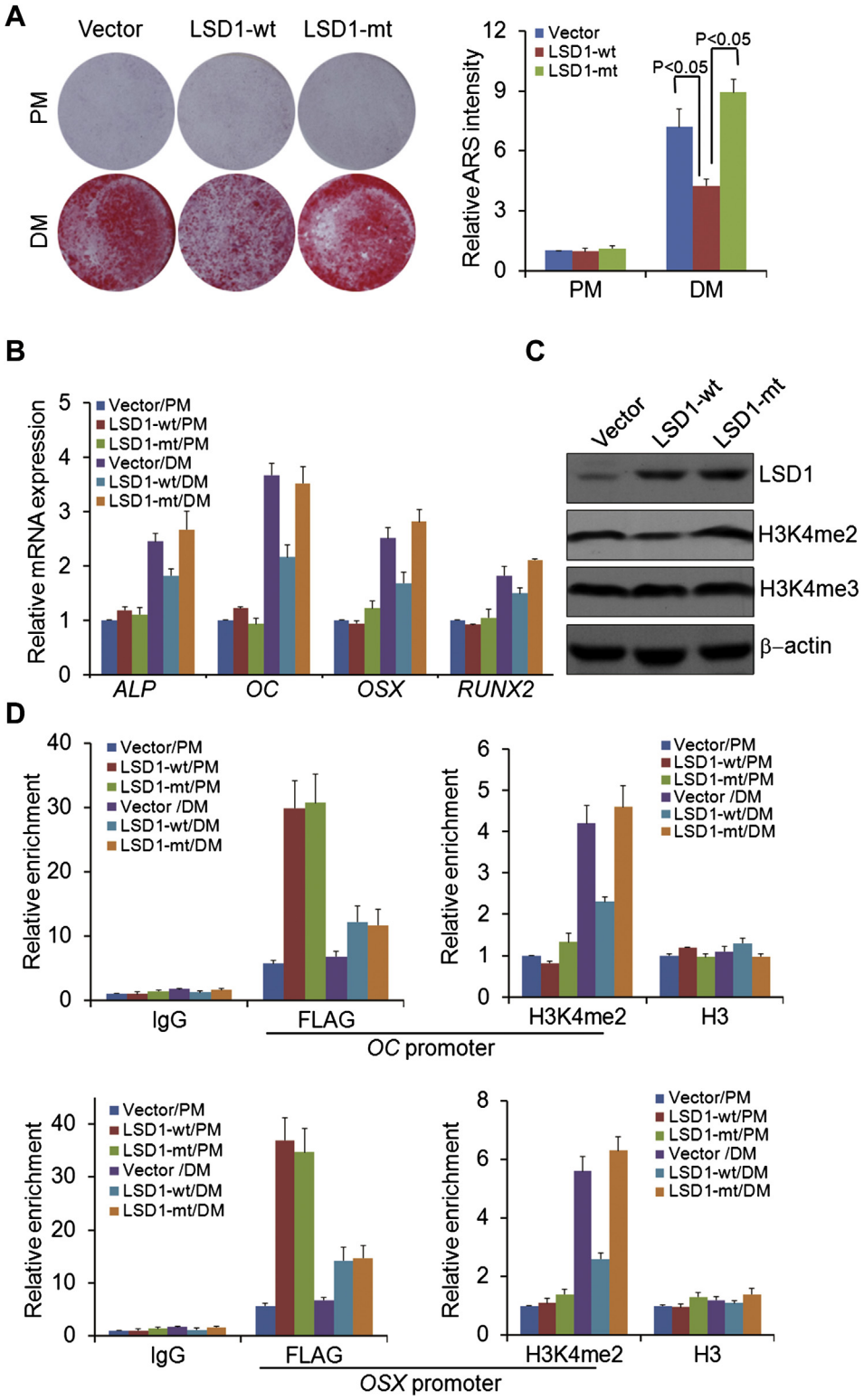

Fig. 4. LSD1 modulates hASCs osteogenic differentiation through its catalytic activity. (A) ARS staining (left panel) and quantification (right panel) of hASCs infected with control, LSD1-wt or LSD1-mt viruses. (B) qRT-PCR analysis of osteogenesis associated genes expression in hASCs infected with control, LSD1-wt or LSD1-mt viruses. (C) Western blotting analysis of the demethylase activity of LSD1-wt and LSD1-mt in hASCs with antibodies as indicated. (D) qChIP analysis of LSD1, H3 and H3K4me2 enrichment on *OC* and *OSX* gene promoters in hASCs infected with control, LSD1-wt or LSD1-mt viruses.

differentiation of hASCs via regulation of osteogenic associated genes.

To solidify our *in vitro* observations, Bio-Oss Collagen transplantation was used to identify the role of LSD1 in an athymic mice xenograft model. Bio-Oss Collagen is a combination of purified cancellous natural bone mineral granules (Bio-Oss) and 10% collagen fibers in a block form which facilitates handling of the graft particles and holds the Bio-Oss Collagen at the desired place. It acts

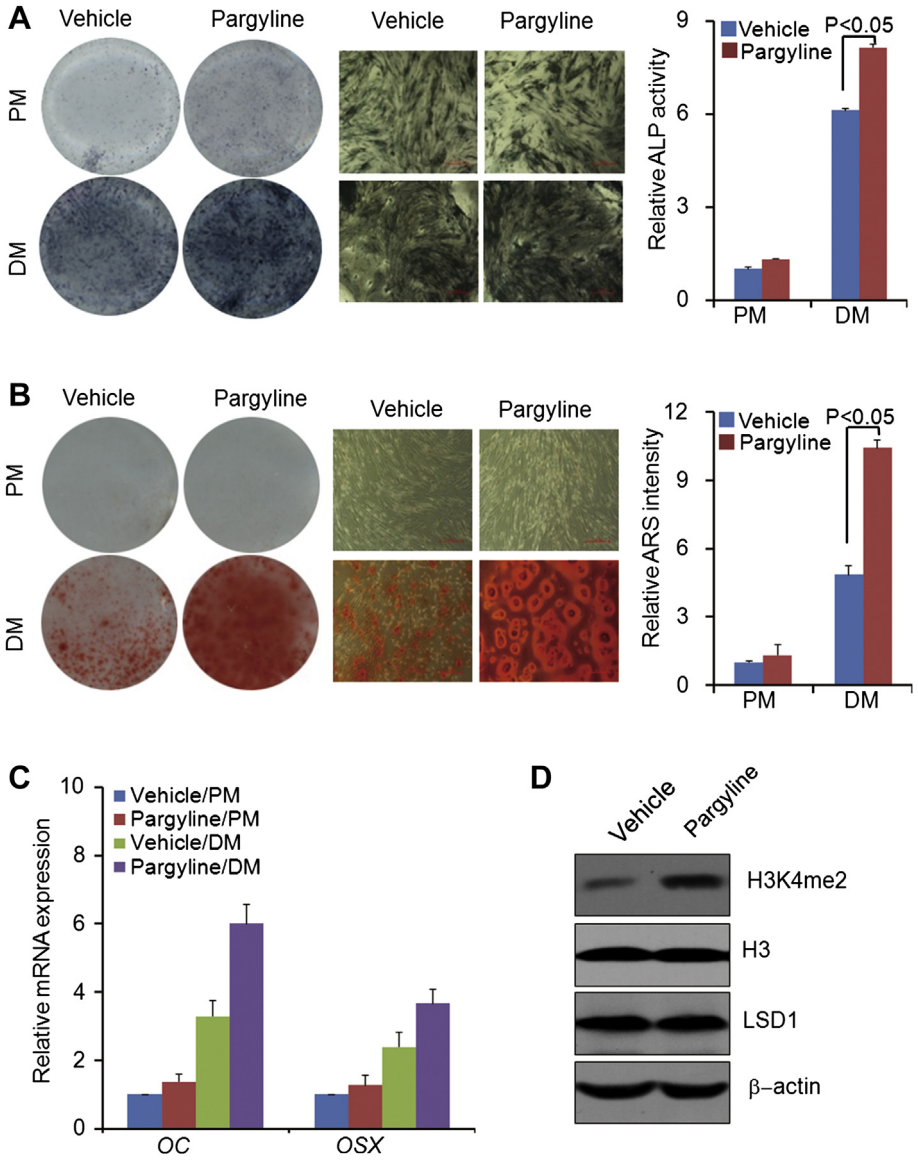

Fig. 5. LSD1 inhibitor pargyline promotes hASCs osteogenic differentiation. (A) ALP staining (left and middle panel) and quantification (right panel) of hASCs in the presence of vehicle or pargyline. (B) ARS staining (left panel and middle panel) and quantification (right panel) of hASCs in the presence of vehicle or pargyline. (C) qRT-PCR analysis of osteogenesis associated genes *OC* and *OSX* expression in the presence of pargyline. (D) Western blotting analysis of the demethylase activity of LSD1 in the presence of pargyline with antibodies as indicated.

as a framework onto which bone-forming cells and blood vessels travel along to construct new bone. Bio-Oss Collagen has been reported to be highly osteoconductive [30]. Taking advantage of this system, the function of LSD1 was determined *in vivo* using x-ray imaging as well as histological and immunological staining.

Emerging evidence suggests that in the absence of differentiation signals, osteogenic genes promoters are occupied by an assembly of transcription repressors such as histone deacetylases (HDACs), transducin-like enhancer of split (TLE) proteins, SIN3 transcription regulator family member A (SIN3A) and Yes-associated protein (YAP) [46–49]. In our previous studies, we demonstrated that jmjc domain containing histone demethylase RBP2 functions to inhibit osteogenic differentiation of hASCs through its H3K4 tri-methyl demethylase activity [12]. H3K4 methylation is a prominent histone mark associated with gene activation, transcription activation and chromatin relaxation, therefore it is logical to imagine that the repression of differentiation associated genes are regulated by protein complexes containing enzymatic activities to erase this mark [41,50]. Since RBP2 and LSD1 preferentially catalyze demethylation of H3K4me3 and H3K4me2, respectively, it will be interesting to investigate whether RBP2 and LSD1 act in a sequential manner or coordinated fashion to regulate osteogenic genes expression and osteogenic process of hASCs.

Recently, several research groups as well as industrial companies have developed more flexible, efficient, and rapid chemical synthesis schemes to identify better compounds targeting LSD1 with high affinity, specificity, cell permeability and stability. Despite LSD1 inhibitors have been widely investigated in medical application of tumor therapy [26,51,52], they have not been used in the bone engineering field. In our study, two types of inhibitors were used to test their influence on osteogenic differentiation of hASCs. Although the monoamine oxidase (MAO) inhibitor pargyline could effectively promote osteogenic differentiation of hASCs,

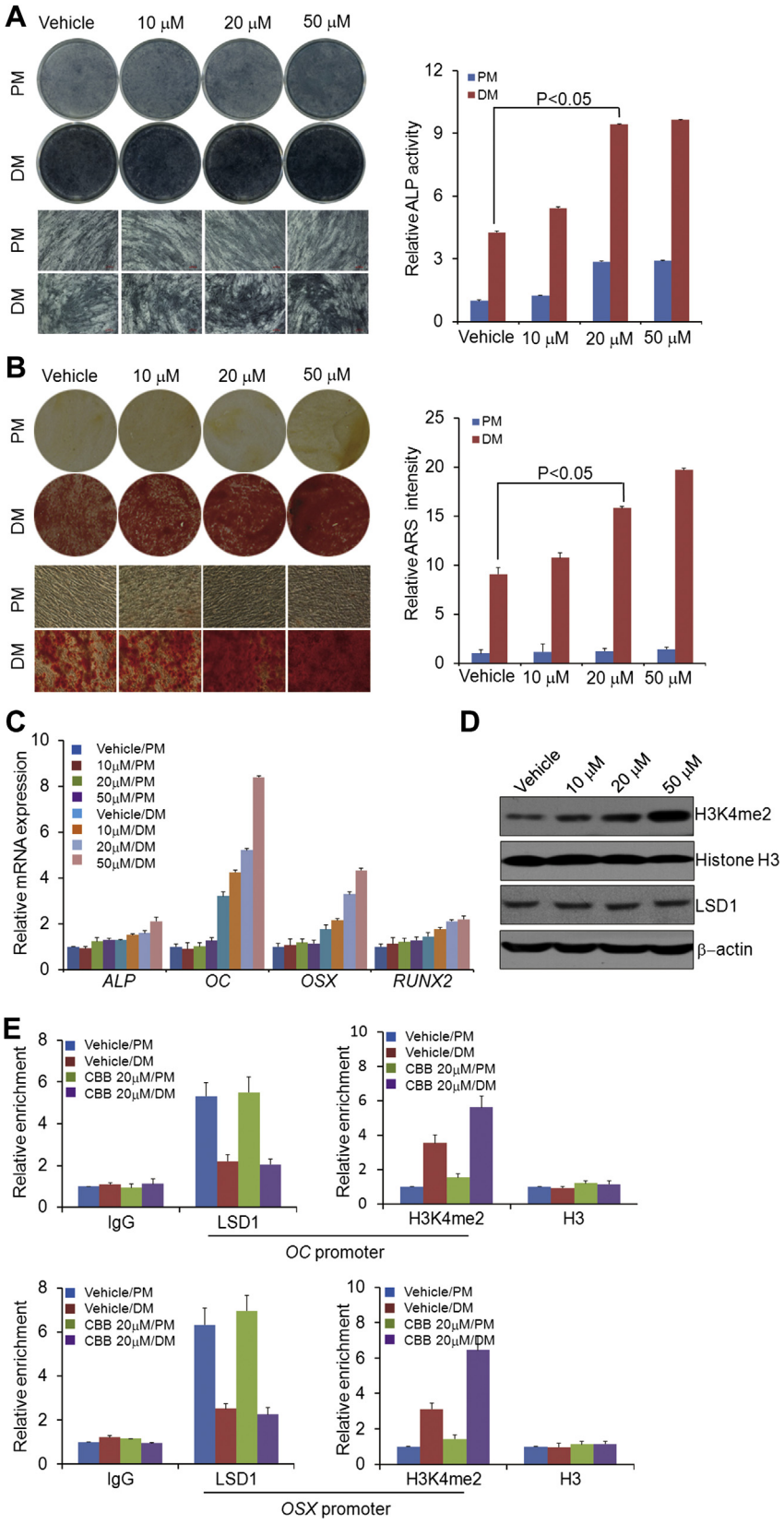

Fig. 6. LSD1 inhibitor CBB1007 promotes hASCs osteogenic differentiation. (A) ALP staining (left and middle panel) and quantification (right panel) of hASCs in the presence of vehicle or CBB1007. (B) ARS staining (left panel and middle panel) and quantification (right panel) of hASCs in the presence of vehicle or CBB1007. (C) qRT-PCR analysis of osteogenesis associated genes expression in the absence or presence of CBB1007. One of the triplicate experiments was shown. (D) Western blotting analysis of the demethylase activity of LSD1 in the presence of CBB1007 with antibodies as indicated. (E) qChIP analysis of LSD1, H3 and H3K4me2 enrichment on *OC* and *OSX* gene promoters in hASCs treated with vehicle or CBB1007.

we realized that its nonselective activity makes our conclusion questionable to some extent. Therefore, CBB1007, an amidinoguanidinium compound that acts as a potent, reversible and substrate competitive LSD1 selective inhibitor [26] was further used to test the influence of LSD1 demethylase activity on osteogenic differentiation. In our study, we demonstrated that this specific bioactive inhibitor of LSD1 could dramatically enhance H3K4 methylation, facilitate de-repression of epigenetically suppressed osteogenic genes, and consequently promote osteogenic differentiation of hASCs. Our findings not only broad the application of LSD1 inhibitors, but provides a new and valuable method in the bone tissue engineering field, although the *in vivo* effect of LSD1 inhibitor remains to be investigated. Currently, it was reported that histone deacetylases (HDACs) inhibitors favored the osteogenic differentiation of mesenchymal stromal/stem cells including hASCs [53–56]. It will be interesting to test whether inhibitors against HDACs and LSD1 could be jointly and synergistically used to regulate osteogenic commitment of hASCs.

In summary, our results demonstrated that LSD1 inhibits osteogenic differentiation of hASCs through its catalytic activity. Our observations not only unravel the functional role of LSD1 in osteogenic differentiation, but also contribute to further understanding how osteogenic genes are regulated in an epigenetic layer. To some extent, we also provide valuable information on how to promote osteogenic differentiation of hASCs in the bone tissue engineering field.

5. Conclusions

In this work, we demonstrated that histone demethylase LSD1 inhibits osteogenic differentiation of hASCs *in vitro* and *in vivo*. Moreover, we found that LSD1 regulates the expression of osteogenesis associated genes largely dependent on its catalytic activity. Interestingly, we revealed that LSD1 inhibitors, especially CBB1007 could be used to efficiently promote osteogenic differentiation of hASCs.

Acknowledgments

This work was supported by grants (81200763 to W.G., 81070809 to Y.Z., 81272284 and 91219102 to L.S) from the National Natural Science Foundation of China, grants from Program for New Century Excellent Talents (NCET) in University from Ministry of Education of China to L.S. (NCET-13-0934) and Y.Z. (NCET-11-0026), a grant from PKU School of Stomatolgy for talented young investigators to W.G and construction program for national key clinical specialty from National Health and Family Planning Commission of China.

References

[1] Zuk PA, Zhu M, Ashjian P, De Ugarte DA, Huang JI, Mizuno H, et al. Human adipose tissue is a source of multipotent stem cells. Mol Biol Cell 2002;13:4279–95.
[2] Levi B, James AW, Nelson ER, Li S, Peng M, Commons GW, et al. Human adipose-derived stromal cells stimulate autogenous skeletal repair via paracrine Hedgehog signaling with calvarial osteoblasts. Stem Cells Dev 2011;20:243–57.
[3] De Toni F, Poglio S, Youcef AB, Cousin B, Pflumio F, Bourin P, et al. Human adipose-derived stromal cells efficiently support hematopoiesis in vitro and in vivo: a key step for therapeutic studies. Stem Cells Dev 2011;20:2127–38.
[4] Hicok KC, Du Laney TV, Zhou YS, Halvorsen YD, Hitt DC, Cooper LF, et al. Human adipose-derived adult stem cells produce osteoid in vivo. Tissue Eng 2004;10:371–80.
[5] Yu LH, Kim MH, Park TH, Cha KS, Kim YD, Quan ML, et al. Improvement of cardiac function and remodeling by transplanting adipose tissue-derived stromal cells into a mouse model of acute myocardial infarction. Int J Cardiol 2010;139:166–72.
[6] Hong L, Peptan IA, Colpan A, Daw JL. Adipose tissue engineering by human adipose-derived stromal cells. Cells Tissues Organs 2006;183:133–40.
[7] Levi B, James AW, Nelson ER, Vistnes D, Wu B, Lee M, et al. Human adipose derived stromal cells heal critical size mouse calvarial defects. PLoS One 2010;5:e11177.
[8] Rada T, Reis RL, Gomes ME. Adipose tissue-derived stem cells and their application in bone and cartilage tissue engineering. Tissue Eng Part B Rev 2009;15:113–25.
[9] Tapp H, Hanley Jr EN, Patt JC, Gruber HE. Adipose-derived stem cells: characterization and current application in orthopaedic tissue repair. Exp Biol Med (Maywood) 2009;234:1–9.
[10] Chung MT, Zimmermann AS, Paik KJ, Morrison SD, Hyun JS, Lo DD, et al. Isolation of human adipose-derived stromal cells using laser-assisted liposuction and their therapeutic potential in regenerative medicine. Stem Cells Transl Med 2013;2:808–17.
[11] Doi A, Park IH, Wen B, Murakami P, Aryee MJ, Irizarry R, et al. Differential methylation of tissue- and cancer-specific CpG island shores distinguishes human induced pluripotent stem cells, embryonic stem cells and fibroblasts. Nat Genet 2009;41:1350–3.
[12] Ge W, Shi L, Zhou Y, Liu Y, Ma GE, Jiang Y, et al. Inhibition of osteogenic differentiation of human adipose-derived stromal cells by retinoblastoma binding protein 2 repression of RUNX2-activated transcription. Stem Cells 2011;29:1112–25.
[13] Sinha KM, Yasuda H, Coombes MM, Dent SY, de Crombrugghe B. Regulation of the osteoblast-specific transcription factor Osterix by NO66, a Jumonji family histone demethylase. EMBO J 2010;29:68–79.
[14] Tao Y, Wu M, Zhou X, Yin W, Hu B, de Crombrugghe B, et al. Structural insights into histone demethylase NO66 in interaction with osteoblast-specific transcription factor Osterix and gene repression. J Biol Chem 2013;288:16430–7.
[15] Whyte WA, Bilodeau S, Orlando DA, Hoke HA, Frampton GM, Foster CT, et al. Enhancer decommissioning by LSD1 during embryonic stem cell differentiation. Nature 2012;482:221–5.
[16] Qureshi AT, Monroe WT, Dasa V, Gimble JM, Hayes DJ. miR-148b-nanoparticle conjugates for light mediated osteogenesis of human adipose stromal/stem cells. Biomaterials 2013;34:7799–810.
[17] Harrison C. Epigenetic drugs: new modulators of readers and erasers. Nat Rev Drug Discov 2013;12:188.
[18] Kaiser J. Epigenetic drugs take on cancer. Science 2010;330:576–8.
[19] Lan F, Nottke AC, Shi Y. Mechanisms involved in the regulation of histone lysine demethylases. Curr Opin Cell Biol 2008;20:316–25.
[20] Shi Y, Lan F, Matson C, Mulligan P, Whetstine JR, Cole PA, et al. Histone demethylation mediated by the nuclear amine oxidase homolog LSD1. Cell 2004;119:941–53.
[21] Williams JS, Chamarthi B, Goodarzi MO, Pojoga LH, Sun B, Garza AE, et al. Lysine-specific demethylase 1: an epigenetic regulator of salt-sensitive hypertension. Am J Hypertens 2012;25:812–7.
[22] Forneris F, Binda C, Battaglioli E, Mattevi A. LSD1: oxidative chemistry for multifaceted functions in chromatin regulation. Trends Biochem Sci 2008;33:181–9.
[23] Kahl P, Gullotti L, Heukamp LC, Wolf S, Friedrichs N, Vorreuther R, et al. Androgen receptor coactivators lysine-specific histone demethylase 1 and four and a half LIM domain protein 2 predict risk of prostate cancer recurrence. Cancer Res 2006;66:11341–7.
[24] Wang J, Scully K, Zhu X, Cai L, Zhang J, Prefontaine GG, et al. Opposing LSD1 complexes function in developmental gene activation and repression programmes. Nature 2007;446:882–7.
[25] Chen Y, Jie W, Yan W, Zhou K, Xiao Y. Lysine-specific histone demethylase 1 (LSD1): a potential molecular target for tumor therapy. Crit Rev Eukaryot Gene Expr 2012;22:53–9.
[26] Wang J, Lu F, Ren Q, Sun H, Xu Z, Lan R, et al. Novel histone demethylase LSD1 inhibitors selectively target cancer cells with pluripotent stem cell properties. Cancer Res 2011;71:7238–49.
[27] Mosammaparast N, Shi Y. Reversal of histone methylation: biochemical and molecular mechanisms of histone demethylases. Annu Rev Biochem 2010;79:155–79.
[28] Greer EL, Shi Y. Histone methylation: a dynamic mark in health, disease and inheritance. Nat Rev Genet 2012;13:343–57.
[29] Shi Y, Whetstine JR. Dynamic regulation of histone lysine methylation by demethylases. Mol Cell 2007;25:1–14.
[30] Wang Y, Zhang H, Chen Y, Sun Y, Yang F, Yu W, et al. LSD1 is a subunit of the NuRD complex and targets the metastasis programs in breast cancer. Cell 2009;138:660–72.
[31] Foster CT, Dovey OM, Lezina L, Luo JL, Gant TW, Barlev N, et al. Lysine-specific demethylase 1 regulates the embryonic transcriptome and CoREST stability. Mol Cell Biol 2010;30:4851–63.
[32] Rudolph T, Beuch S, Reuter G. Lysine-specific histone demethylase LSD1 and the dynamic control of chromatin. Biol Chem 2013;394:1019–28.
[33] Adamo A, Sese B, Boue S, Castano J, Paramonov I, Barrero MJ, et al. LSD1 regulates the balance between self-renewal and differentiation in human embryonic stem cells. Nat Cell Biol 2011;13:652–9.
[34] Kerenyi MA, Shao Z, Hsu YJ, Guo G, Luc S, O'Brien K, et al. Histone demethylase Lsd1 represses hematopoietic stem and progenitor cell signatures during blood cell maturation. Elife 2013;2:e00633.

[35] Neelamegam R, Ricq EL, Malvaez M, Patnaik D, Norton S, Carlin SM, et al. Brain-penetrant LSD1 inhibitors can block memory consolidation. ACS Chem Neurosci 2012;3:120–8.
[36] Pollock JA, Larrea MD, Jasper JS, McDonnell DP, McCafferty DG. Lysine-specific histone demethylase 1 inhibitors control breast cancer proliferation in ERalpha-dependent and -independent manners. ACS Chem Biol 2012;7:1221–31.
[37] Liang Y, Quenelle D, Vogel JL, Mascaro C, Ortega A, Kristie TM. A novel selective LSD1/KDM1A inhibitor epigenetically blocks herpes simplex virus lytic replication and reactivation from latency. MBio 2013;4. e00558-12.
[38] Lynch JT, Harris WJ, Somervaille TC. LSD1 inhibition: a therapeutic strategy in cancer? Expert Opin Ther Targets 2012;16:1239–49.
[39] Shang Y, Hu X, DiRenzo J, Lazar MA, Brown M. Cofactor dynamics and sufficiency in estrogen receptor-regulated transcription. Cell 2000;103:843–52.
[40] Shang Y, Brown M. Molecular determinants for the tissue specificity of SERMs. Science 2002;295:2465–8.
[41] Shi L, Sun L, Li Q, Liang J, Yu W, Yi X, et al. Histone demethylase JMJD2B coordinates H3K4/H3K9 methylation and promotes hormonally responsive breast carcinogenesis. Proc Natl Acad Sci U S A 2011;108:7541–6.
[42] Murray-Stewart T, Woster PM, Casero Jr RA. The re-expression of the epigenetically silenced e-cadherin gene by a polyamine analogue lysine-specific demethylase-1 (LSD1) inhibitor in human acute myeloid leukemia cell lines. Amino Acids 2014;46:585–94.
[43] Murphy DL, Karoum F, Pickar D, Cohen RM, Lipper S, Mellow AM, et al. Differential trace amine alterations in individuals receiving acetylenic inhibitors of MAO-A (clorgyline) or MAO-B (selegiline and pargyline). J Neural Transm Suppl 1998;52:39–48.
[44] Metzger E, Wissmann M, Yin N, Muller JM, Schneider R, Peters AH, et al. LSD1 demethylates repressive histone marks to promote androgen-receptor-dependent transcription. Nature 2005;437:436–9.
[45] Liang Y, Vogel JL, Narayanan A, Peng H, Kristie TM. Inhibition of the histone demethylase LSD1 blocks alpha-herpesvirus lytic replication and reactivation from latency. Nat Med 2009;15:1312–7.
[46] Lamour V, Detry C, Sanchez C, Henrotin Y, Castronovo V, Bellahcene A. Runx2- and histone deacetylase 3-mediated repression is relieved in differentiating human osteoblast cells to allow high bone sialoprotein expression. J Biol Chem 2007;282:36240–9.
[47] Westendorf JJ. Transcriptional co-repressors of Runx2. J Cell Biochem 2006;98:54–64.
[48] Jensen ED, Nair AK, Westendorf JJ. Histone deacetylase co-repressor complex control of Runx2 and bone formation. Crit Rev Eukaryot Gene Expr 2007;17:187–96.
[49] Ali SA, Zaidi SK, Dobson JR, Shakoori AR, Lian JB, Stein JL, et al. Transcriptional corepressor TLE1 functions with Runx2 in epigenetic repression of ribosomal RNA genes. Proc Natl Acad Sci U S A 2010;107:4165–9.
[50] Pekowska A, Benoukraf T, Zacarias-Cabeza J, Belhocine M, Koch F, Holota H, et al. H3K4 tri-methylation provides an epigenetic signature of active enhancers. EMBO J 2011;30:4198–210.
[51] Yu Y, Wang B, Zhang K, Lei Z, Guo Y, Xiao H, et al. High expression of lysine-specific demethylase 1 correlates with poor prognosis of patients with esophageal squamous cell carcinoma. Biochem Biophys Res Commun 2013;437:192–8.
[52] Huang Y, Vasilatos SN, Boric L, Shaw PG, Davidson NE. Inhibitors of histone demethylation and histone deacetylation cooperate in regulating gene expression and inhibiting growth in human breast cancer cells. Breast Cancer Res Treat 2012;131:777–89.
[53] Cho HH, Park HT, Kim YJ, Bae YC, Suh KT, Jung JS. Induction of osteogenic differentiation of human mesenchymal stem cells by histone deacetylase inhibitors. J Cell Biochem 2005;96:533–42.
[54] Hu X, Zhang X, Dai L, Zhu J, Jia Z, Wang W, et al. Histone deacetylase inhibitor trichostatin A promotes the osteogenic differentiation of rat adipose-derived stem cells by altering the epigenetic modifications on Runx2 promoter in a BMP signaling-dependent manner. Stem Cells Dev 2013;22:248–55.
[55] Maroni P, Brini AT, Arrigoni E, de Girolamo L, Niada S, Matteucci E, et al. Chemical and genetic blockade of HDACs enhances osteogenic differentiation of human adipose tissue-derived stem cells by oppositely affecting osteogenic and adipogenic transcription factors. Biochem Biophys Res Commun 2012;428:271–7.
[56] Shakibaei M, Shayan P, Busch F, Aldinger C, Buhrmann C, Lueders C, et al. Resveratrol mediated modulation of Sirt-1/Runx2 promotes osteogenic differentiation of mesenchymal stem cells: potential role of Runx2 deacetylation. PLoS One 2012;7:e35712.